Determination of local active tectonics regime in central and northern Greece, using primary geodetic data

Christos Pikridas[1], Ilias Lazos[2], Alexandros Chatzipetros[3], Spyros Pavlides[4]

[1] Department of Geodesy and Surveying, School of Rural and Surveying Engineering, Aristotle University, 541 24, Thessaloniki, (cpik@topo.auth.gr)
[2] Department of Geology, School of Geology, Aristotle University, 541 24, Thessaloniki, (ilialazo@geo.auth.gr)
[3] Department of Geology, School of Geology, Aristotle University, 541 24, Thessaloniki, (ac@geo.auth.gr)
[4]Department of Geology, School of Geology, Aristotle University, 541 24, Thessaloniki, (pavlides@geo.auth.gr)

Key words: *active tectonics*; *geodynamics*; *triangulation methodology*; *geodetic data*; *GPS stations*; *Central – Northern Greece*

ABSTRACT

Numerous active fault zones are observed throughout the central and northern part of Greece, while in some cases they are related to destructive earthquakes. The geometric characteristics of these fault zones vary, revealing both extensional and compressional tectonics of these structures. The use of geodetic data, received by permanently installed GPS stations, is a precise way of analyzing the tectonic regime. In particular, 58 permanent GPS stations are included in the study area, having collected primary data for a 7-year period. The calculated East and North velocity components and their errors, respectively, derived from each GPS station, were processed applying a triangulation methodology, based on the triangle construction, combining three different GPS stations each time. The use of dense GPS stations distribution resulted in the extraction of 1,092 different triangles and then, the centroid of each triangle was determined. For each centroid the following parameters were estimated: 1) maximum horizontal extension, 2) total velocity, 3) maximum shear strain, 4) area strain and 5) rotation. The extracted values were interpolated into a grid pattern, showing low to medium values, especially north of the inferred extension of the North Aegean Fault System, the same parameter values are high for the southern part of Greece, confirming the geological and seismological data suggesting that Central – Northern Greece is generally less active than Southern Greece. However, it is noted that the length of the neotectonic faults in the area are capable of producing significant earthquakes, albeit in longer recurrence intervals.

I. INTRODUCTION

The aim of the paper is the examination of the tectonic setting of Central – Northern Greece, based on the results derived from the primary geodetic data processing. The neotectonic regime of the study area has been studied by various authors (Sboras et al 2017; Koukouvelas and Aydin, 2002; Mercier et al., 1989; Robertson and Dixon, 1984; Le Pichon and Angelier, 1979), while the neotectonic and seismological research led to the conclusion that the study area has been affected by the N – S extensional regime, initiated during Late Miocene – Pliocene, resulted in the occurrence of E – W, normal active fault zones (Mountrakis et al., 2006).

In addition the aforementioned extensional tectonics caused the reactivation of inactive, older than Miocene normal fault zones, striking both NW – SE and NE – SW. Therefore, all of the fault zones are associated with the grabens and horsts, documented throughout the study area (Mountrakis, 2006). Furthermore, it is mentioned that the North Aegean Trough fault zone, as well as Ionian Sea fault zones (mainly the Lefkada and Cephalonia fault zones) are characterized as strike-slip fault zones.

Regarding the historical seismicity of the area, numerous earthquake events have been recorded. Figure 1 shows the major composite and individual seismogenic sources, based on the Greek Database of Seismogenic Sources (GreDaSS) (Caputo et al., 2013; Sboras, 2012; Pavlides et al., 2010)

Some typical examples of recent earthquake events within the Central – Northern Greece are the following: a) the M_w6.4 Lefkada Island seismic event of 17 November 2015 (Sboras et al., 2016), b) the M_w6.5 Kozani – Grevena seismic event of 13 May 1995 (Pavlides et al., 1995), c) the M_w6.0 Goumenissa seismic event of 21 December 1990 (Panagiotopoulos et al., 1993), d) the M_w6.5 Thessaloniki seismic event of 20 June 1978 (Mercier et al., 1983), e) the M_w6.3 Larisa seismic event of 1 March 1941 (Caputo, 1995) and f) the M_w7.0 Ierissos seismic event of 26 September 1932 (Chatzipetros et al., 2005; Pavlides and Tranos 1991).

Figure 1 The Composite (orange boxes) and Individual (yellow boxes) Seismogenic Sources of the study area, according to the Greek Database of Seismogenic Sources (GreDaSS) (modified from Caputo et al., 2013; Sboras, 2012; Pavlides et al., 2010)

II. GPS DATA AND ANALYSIS SCHEME

In the last two decades the GNSS measurements are widely used as a well-established tool in earth crustal deformation studies. Hence, the synergy between geodesy and geophysics can provide some very promising discussion about the Earth's crustal processes.

In this paper, we use a subset of the geodetic velocities which are provided by a previous study of Bitharis et al. (2016). We focus on the broader region of Central and Northern Greece, including 58 GPS permanent stations with dense distribution in order to estimate the deformation parameters. GPS stations are part of HxGN/SmartNet Greece, NoaNet, Hepos, and HermesNet Fotiou et al. (2010) permanent Networks. In addition, EPN stations are also included.

The geodetic velocities are referred on European Terrestrial Reference Frame 2000 (ETRF2000), which practically is coincident with the stable part of the Eurasian Plate. It should be mentioned that geodetic velocities were based on 7 years continuously 24-hourly operating GNSS data (2008-2014).

In our processing about the GNSS data analysis we apply all the recommendations from the analysis centers (e.g. EUREF). We use the Vienna Mapping Function 1 (VMF1), (Boehm et al., 2006), in order to estimate the Zenith Total Delay (ZTD) with two hours interval. Also, for the long-term analysis we follow the IERS2003 conventions, concerning to Solid Earth Tides. The whole GNSS processing has carried out with GAMIT/GLOBK (Herring et al., 2010) software suite (release 10.5). The initial phase ambiguities of carrier frequencies were resolved at high percentage level. As it is known, carrier phase data are biased by an integer number of carrier wavelengths which called initial phase ambiguity and must be estimated from the data. If phase ambiguity resolution is succeeded, then high accuracy results are obtained. Figure 2 shows the resolution percentage for wide lane and narrow lane ambiguity of network baselines during processing.

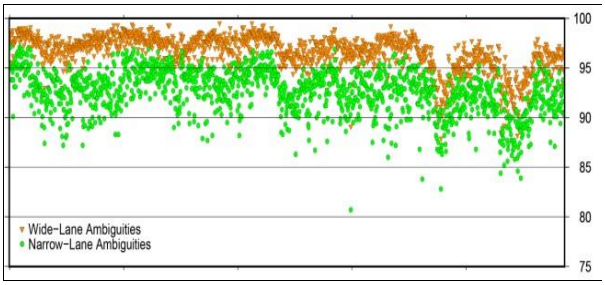

Figure 2. Resolution percentage for wide lane and narrow lane ambiguities.

III. TRIANGULATION METHODOLOGY

The calculation of parameters, including maximum horizontal extension, total velocity, maximum shear strain, area strain and rotation, is based on the triangulation methodology. The principal of this methodology is the combination of the primary raw geodetic data of three different GPS stations each time, forming a triangle (Lazos et al., 2018a). In particular, each of the three GPS stations is located on a triangle vertex, respectively, forming an imaginary triangle, while each station is characterized by an East and North velocity component and their errors, respectively, determined by the primary raw data processing.

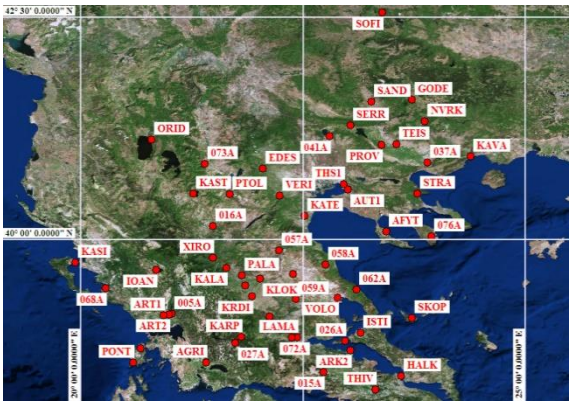

Figure 3. 58 permanently installed GPS stations (red dots), distributed into the study area.

Initially, the three triangle medians determine the triangle centroid, which is considered as the starting point (0, 0) of a new coordinate system. Then, an inner circle is designed into the original and undeformed triangle, while the translation vector value is calculated for the triangle centroid, taking into account all three total horizontal velocities. The triangle vertices position changes, due to the relocation of each vertex from the starting to the finishing point of each total horizontal velocity vector, causing the transformation of the circle into an ellipse, while the undeformed and the deformed triangle centers are connected by the translation vector at the same time. Subtracting the translation vector from all three total horizontal velocity vectors leads to the relocation of the deformed triangle centroid to the starting point (0, 0), where the centroid of the undeformed centroid is also located (Lazos et al., 2018a).

Regarding the formation of the ellipse, a major and a minor axis, perpendicular to each other, are determined, while the relocation of the deformed triangle into the original position leads to the ellipse transformation into a circle, while the ellipse maintains the same axes. The implementation of this process, using different mathematical equations, including the original and final lengths of the ellipse axes, leads to the estimation of the aforementioned parameters. In the present paper, the GPS triangulation process is based on the GPS triangular calculator software, developed by the UNAVCO (http://www.unavco.org).

As it was mentioned above, 58 permanently installed GPS stations are included within the study area (Figure 3), recording the primary geodetic data and therefore, the combinations between the GPS stations are numerous. In particular, the dense GPS stations network of the study area resulted in the construction of 1,092 different triangles, while all five aforementioned parameters were calculated for the 1,092 different triangle centroids (Figure 4).

IV. Results

A. *Maximum horizontal extension*

The maximum horizontal extension is one of the most reliable indicators of confirming tectonically active structures in a study area. The direction of the maximum horizontal extension vectors is perpendicular to the strike of the tectonically active structure (e.g active fault zones), while their values, combined with the general tectonic regime of the area, reveal an extensional or a compressional type of tectonics, associated with normal, reverse or strike-slip faulting.

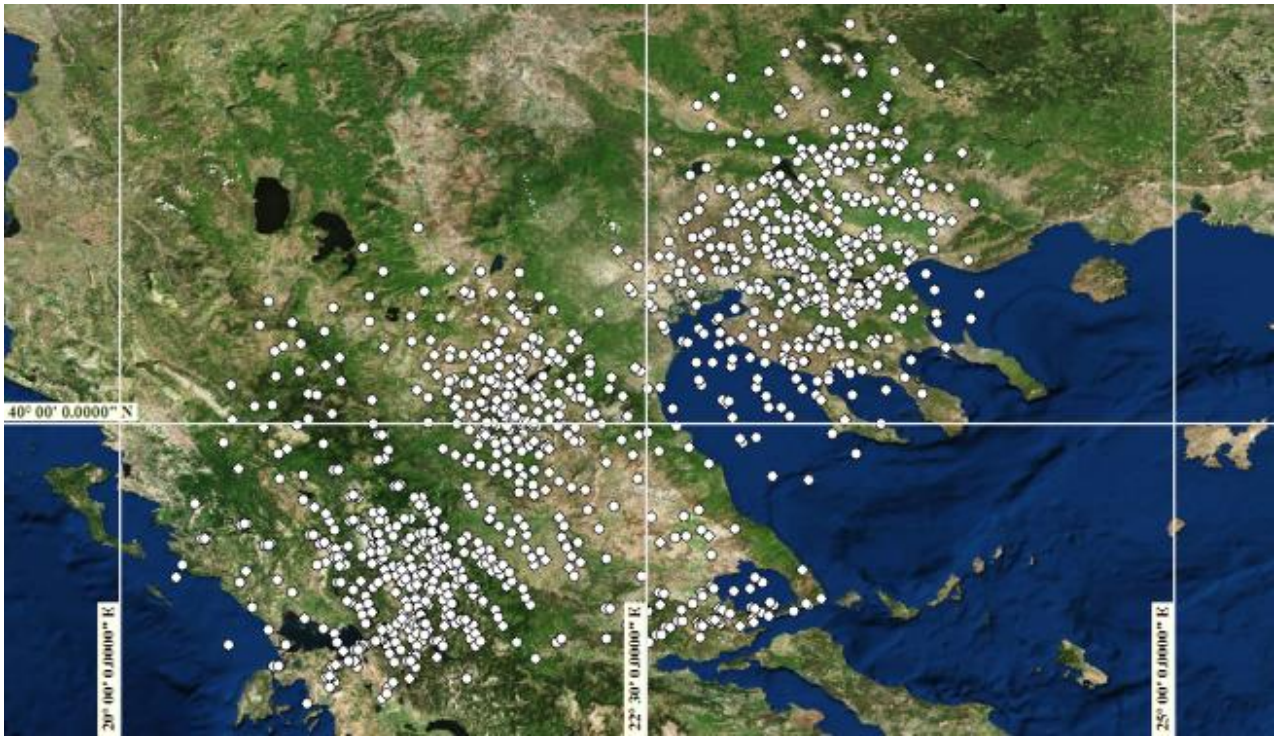

Figure 4. 1,092 different triangle centroids (white dots) of the study area, derived from the combination of the 58 permanently installed GPS stations. For each of them maximum horizontal extension, total velocity, maximum shear strain, area strain and rotation were calculated

The maximum horizontal extension (MHE) is calculated by the equation:

$$MHE = (l_f - l_0)/l_0 \quad (1)$$

where l_f = the final length along the longest axe of the strain ellipse

l_0 = the original length along the longest axe of the strain ellipse

Considering the total of the 1,092 different maximum horizontal extension values, interpolation methodology (kriging) was applied, extracting a grid pattern, including the maximum horizontal extension values distribution (Figure 5).

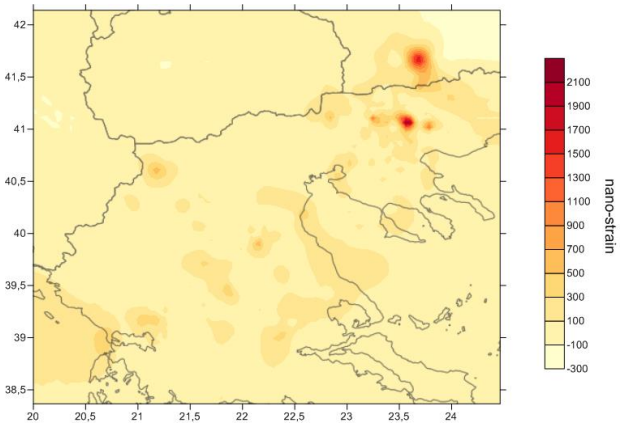

Figure 5. Interpolation of the maximum horizontal extension values of the study area

The extracted results of maximum horizontal extension values (ranging mainly between -100 and 500 nano-strain) confirm the limited tectonic activity of the central and northern part of Greece, compared to the southern part. Two locations present remarkably high maximum horizontal extension values at the northeastern part of the study area, caused mainly by insignificant seismic events or local creeping phenomena. Beside these two locations, the systematically highest values are presented at the western – southwestern part of the study area, where the active, seismic, strike-slip fault of Lefkada Island is identified, as well as at the eastern part of Thessaly area, affected both by the confirmed active fault zones of Larisa plain and the southwestern prolongation of North Anatolian fault zone.

B. *Total velocity*

Total velocity is the parameter, expressing the geotectonic evolution of a study. Various authors (Hollenstein et al., 2008; Reilinger et al., 2006; McClusky et al., 2000) have determined the motion of the Greek – Turkish area, showing the concentration of the highest velocity values at the close area of subduction zone, where African plate is subducted beneath the Eurasian.

The estimation of total velocity (TV) is based on the application of the Pythagorean Theorem and is extracted by the following equation:

$$TV = \sqrt{N^2 + E^2} \quad (2)$$

where N= the north velocity component

E= the east velocity component

Based on the centroids of the constructed triangles, the total velocity vectors were designed, showing a systematic motion, ranging mainly between a N – S direction at the northern – northeastern part and a NE – SW direction at the southern – southwestern part of the study area (Figure 6).

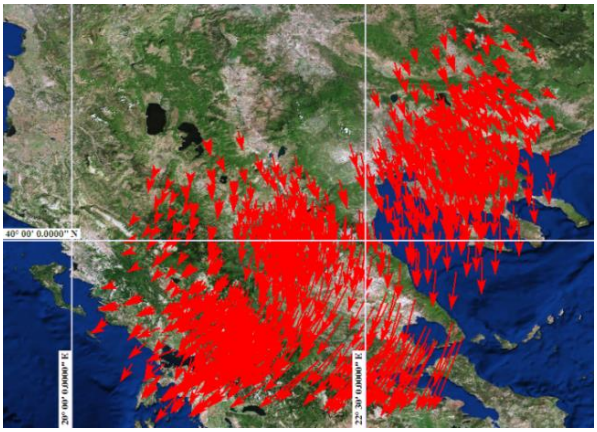

Figure 6 Total velocity vectors of the study area.

The interpolated results of total velocity (Figure 7) show the increase of values from the northern (0.002 m/yr) to the southern (0.019 m/yr) part of the study area. Furthermore, the combination of these values with the aforementioned directions confirms the high total velocity values at the close area of the subduction zone.

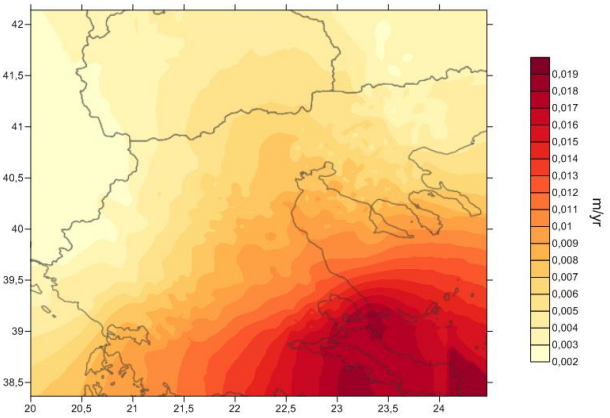

Figure 7. Interpolation of the total velocity values of the study area

C. *Maximum shear strain*

The maximum shear strain parameter is an important indicator of detecting active fault zones, as in many cases shearing is directly associated with the faults motion (Hackl et al., 2009). Mathematically, the

maximum shear strain (MSS) is calculated by the equation:

$$MSS = e_{1H} - e_{2H} \quad (3)$$

where e_{1H}= the extension along the major axis (S_{1H}) of the ellipse

e_{2H}= the extension along the minor axis (S_{2H}) of the ellipse

The results of the maximum shear strain interpolation (Figure 8) confirm the tectonically inactive character of the study area, in contrast with the southern part of Greece. Furthermore, high maximum shear strain values appear in the same way with the maximum horizontal extension values at the northeastern (2,000 nano-strain) part of the area. Additionally, an area of high maximum shear strain value is observed at the southwestern part of the study area, caused probably by the triggering of landslide phenomena.

However, in Figure 8 the high maximum shear strain activity (2,800 nano-strain) in the northern part of the Ionian Sea region is presented, associated with the occurrence of the 2015 destructive seismic event of Lefkada Island.

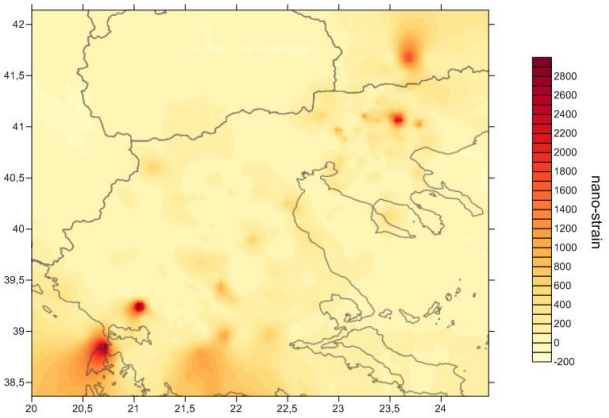

Figure 8. Interpolation of the maximum shear strain values of the study area.

D. *Area strain*

Area strain is a parameter of determining the type of tectonic regime of an area. In particular, the kinds of area strain, extracted by the implementation of the triangulation methodology are: a) dilatation and b) compaction. Dilatation expresses the increase of an area, associated with an extensional regime, while on the other hand compaction is related to a compressional regime. Therefore, the dilatation of an area is mainly associated with normal faults, as well as with transtensional strike-slip structures, while the compaction of an area is mainly related to reverse faults, as well as with transpressional strike-slip structures.

The calculation of the area strain (AS) is based on the following equation:

$$AS = e_{1H} + e_{2H} \quad (4)$$

where e_{1H}= the extension along the major axis (S_{1H}) of the ellipse

e_{2H}= the extension along the minor axis (S_{2H}) of the ellipse

Taking into account the extracted area strain results, 66 per cent of the triangle centroids show dilatation, while the compaction is presented by the 34 per cent of the triangle centroids, respectively. Therefore, the study area is dominated by an extensional regime, while the area, where compaction is recorded, is more likely to be associated with transpressional strike-slip structures than reverse faulting. In particular, as it is shown in Figure 9, dilatation and compaction coexist at the southwestern part of the study area, where strike-slip structures have been confirmed (Lefkada Island seismic fault), while the same phenomenon is documented at the northeastern part of the study area (Thessaloniki and Chalkidiki area), where the presence of NW – SE strike-slip faults is considered possible. Regarding the compaction, related to reverse faulting, Pindos mountain range (southern part of the study area) is the only part of the study area, where this phenomenon is observed, while it is worth noting that the prolongation of Pindos mountain range into the Albania area is associated with active reverse fault zones. Finally, the observed compaction at the western – northwestern part of Larisa plain is probably related to local structures, as neither reverse faults nor strike-slip zones have been recorded into this part of the study area.

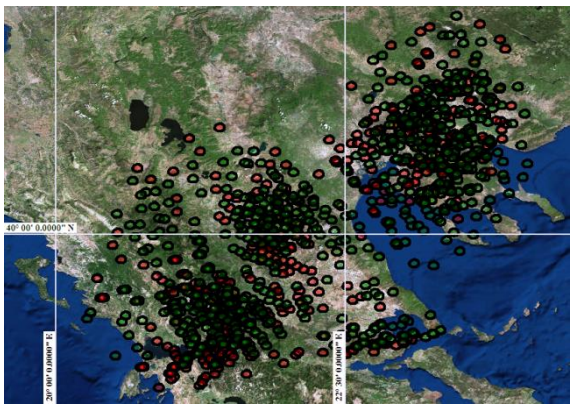

Figure 9. Area strain ellipses, showing dilatation (green ellipses) and compaction (red ellipses) of the study area.

The interpolated results (Figure 10), showing the area strain distribution, reveal the low tectonic activity of the study area, as its major part presents area strain values, ranging between -200 and 200 nano-strain. The remarkably high values are observed, as in the aforementioned parameters, at the northeastern part and the southwestern part (Ionian Sea) of the study area.

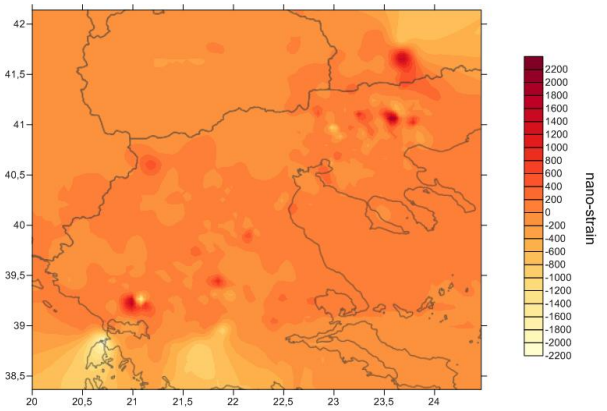

Figure 10. Interpolation of the area strain values of the study area.

E. *Rotation*

Rotation is a parameter, associated with the geodynamic setting, as it shows the orientation and the geotectonic evolution of the study area. The type (clockwise or counter-clockwise) and the rate are decisive for determining the rotation. Based on the triangulation methodology, the annual rotation rate of the 1,092 triangle centroids was estimated. However, the extracted results had no physical importance, as the annual rotation rate is limited (e.g 2×10^{-6} degrees/year), while there is also serious visualization problem of these results.

The aforementioned problems led to the modelling construction, based on the extrapolated values, derived by the annual rotation rates, considering that these rates are stable for the entire time period of each model. Therefore, the models of the next 5 and 10 Myr, respectively, were constructed, in order to be determined the future geotectonic regime. It is mentioned that the construction of a model, referred to a period of the past, can be combined and compared with palaeomagnetic data, determining precisely the type and the rotation rate (Lazos et al., 2018b).

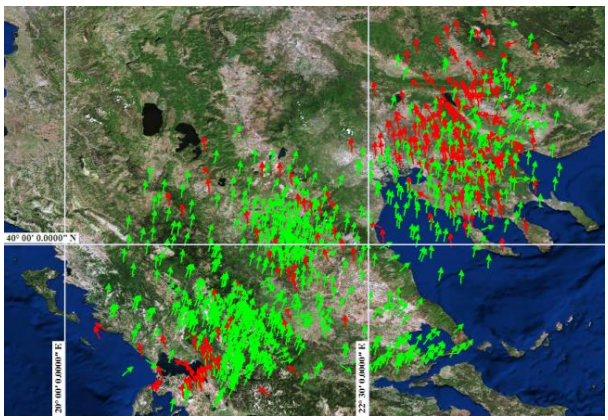

Figure 11. Clockwise (green) and counter-clockwise (red) rotation vectors of the study area for the next 5 Myr period.

The recorded results show that the 65 per cent of the triangle centroids rotates clockwise, while the 35 per cent of them rotates counter-clockwise, respectively, in both 5 Myr (Figure 11) and 10 Myr (Figure 12) models.

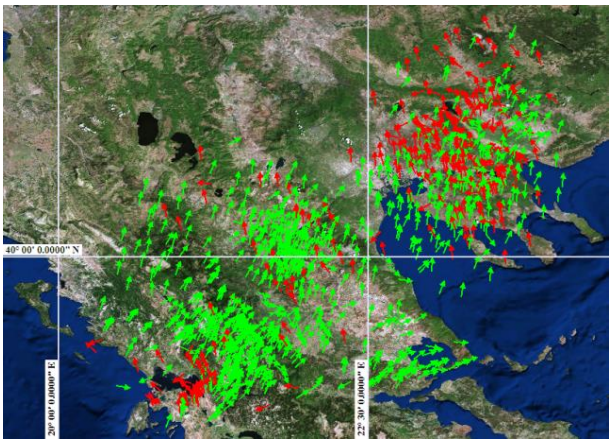

Figure 12. Clockwise (green) and counter-clockwise (red) rotation vectors of the study area for the next 10 Myr period.

The examination of models reveals the dominant clockwise rotation of western, central and northern part of the study area. On the other hand, the counter-clockwise rotation is observed mainly at the northeastern and the southwestern part of the study area. In both parts, the counter-clockwise vectors coexist with clockwise vectors. This combination of both kinds of rotation vectors is an indicator of strike-slip faulting. Therefore, the possible presence of strike-slip fault zones at the aforementioned parts of the study area is also confirmed by the examination of rotation.

The interpolation methodology, applied in the extrapolated rotation values of two models, show the clear and dominant clockwise rotation of Central – Northern Greece. The estimated values of the clockwise rotation of the study area for the next 5 Myr range mainly between 10 and 60 degrees, while the counter-clockwise rotation values between 10 and 40 degrees, respectively (Figure 13).

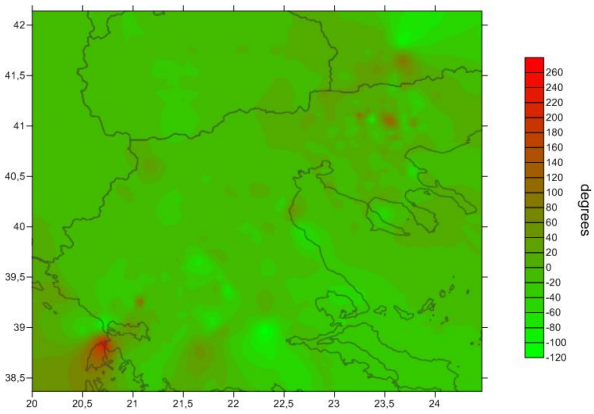

Figure 13. Interpolation of rotation values of the study area for the next 5 Myr period.

Similarly, the clockwise rotation values of the next 10 Myr model (Figure 14) range between 20 and 60 degrees, proving the fact that although the study area rotates in a clockwise way, the rotation rate is limited

and therefore the area can be characterized as practically stable. The counter-clockwise rotation values of this model also range mainly between 10 and 40 degrees.

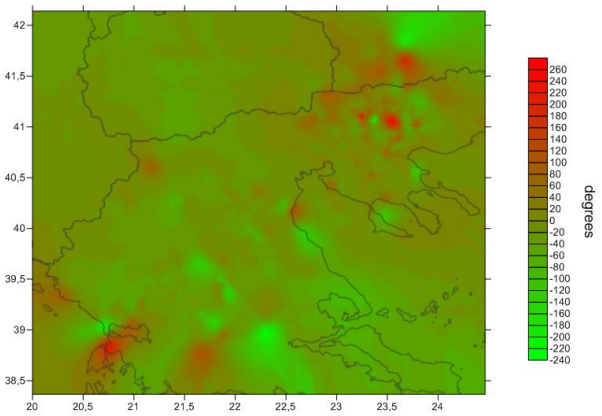

Figure 14. Interpolation of rotation values of the study area for the next 10 Myr period.

V. Discussion and Conclusions

The use of primary geodetic data is one of the most reliable ways of examining and interpreting the tectonic setting and the geotectonic evolution of an area. The study area includes the central and northern part of Greece, where 58 permanently installed GPS stations are located, collecting the geodetic data, using Eurasia as a fixed reference frame. The processing of the primary geodetic data (East and North velocity component) includes the implementation of the triangulation methodology. During this methodology, three different GPS stations are combined each time, forming a triangle. The total of the constructed triangles is 1,092. For each of them, a series of parameters (maximum horizontal extension, total velocity, maximum shear strain, area strain and rotation) is calculated. The analysis of these parameters leads to the evaluation of the tectonic setting.

Initially, the parameter analysis reveals that the study area is generally a tectonically inactive area, in contrast with the southern part of Greece, where a totally different tectonic regime is observed. The major tectonic structure on each side of which the tectonic differentiation is observed, is the North Anatolian fault zone and its prolongation. At the northern part of this fault zone is extended the study area, characterized by the inactive tectonic setting, while at the southern part remarkable tectonically active areas are documented such as South Aegean region, Corinth Gulf etc.

In addition, the maximum horizontal extension analysis confirms significant tectonic structures of the study area, including the Lefkada Island seismic fault, associated with the strong earthquake occurred in 2015. However, all other confirmed tectonic structures do not present important tectonic activity.

Regarding the examination of total velocity, the study area shows a systematic motion to the subduction zone of Eurasia and African plates, being in agreement with various authors. The rate of total velocity increases at the southern part of the study area, as the distance from the subduction zone decreases. It is noted that the corresponding values at Southern Greece are much higher, confirming the important tectonic activity.

The parameter of maximum shear strain certifies both the activation of the seismic fault of Lefkada Island, as well as the lack of tectonic activity in the greatest part of the study area. On the other hand, the analysis of area strain (dilatation or compaction) confirms the normal, reverse and strike-slip fault zones of the area. Furthermore, it is extracted the conclusion that the Lefkada seismic fault is a strike-slip fault, while at the same time the coexistence of dilatation and compaction at the northeastern part of the study area reveals the existence of NW – SE strike-slip structures, almost perpendicular to the North Anatolian fault zone.

Finally, the construction of rotation models of the next 5 and 10 Myr, respectively, show a dominant clockwise rotation, while the counter-clockwise rotations are limited. The presence of both clockwise and counter-clockwise rotations at the Ionian Sea and the northeastern part of the study area verifies the existence of strike-slip fault zones. It is mentioned that the combination of this type of rotation models with palaeomagnetic data can determine the evolution of the exact rotation pattern of a study area.

VI. Acknowledgements

The authors would like to thank the Metrica S.A, National Cadastre and Mapping Agency S.A, National Observatory of Athens (Ganas et al. 2011) and National Technical University of Athens for providing GPS data.

References

Bitharis, S., Fotiou, A., Pikridas, C., andRossikopoulos, D. (2016). A New Velocity Field of Greece Based on Seven Years (2008-2014) Continuously Operating GPS Station Data. Springer Berlin Heidelberg, pp 1-9.

Boehm, J., Werl, B., Schuh, H. (2006). Troposphere mapping functions for GPS and very long baseline interferometry from European Centre for Medium-Range Weather Forecasts operational analysis data. J. Geophys. Res. Solid Earth 111. doi:10.1029/2005JB003629

Caputo, R., Chatzipetros, A., Pavlides, S. and Sboras, S. (2013). The Greek Database of Seismogenic Sources (GreDaSS): state-of-the-art for northern Greece, Ann. Geophys., 55(5), pp 859-894.

Caputo, R. (1995). Inference of a seismic gap from geological data: Thessaly (Central Greece) as a case study. Ann. di Geofis. 38, pp 1–19.

Chatzipetros, A., Michailidou, A., Tsapanos, T., Pavlides, S. (2005). Morphotectonics and seismotectonics of the

Stratoni-Barbara and Gomati-MegaliPanagia active fault (Eastern Chalkidiki, Northern Greece). Bull. Geol. Soc. Greece XXXVII, pp 127–142.

Fotiou, A.,Pikridas,C., Rossikopoulos,D., Spatalas, S., Tsioukas, V., and Katsougiannopoulos, S. (2010). The Hermes GNSSNtripCaster of AUThBollettino di Geodesia et ScienzeAffini,LXIX(1), pp 35 – 43.

Ganas, A., Chousianitis, K., Drakatos, G., Papanikolaou, M., Argyrakis, P., Kolligri, M., Petrou, P., Batsi, E., Tsimi, C. (2011). NOANET: High-rate GPS Network for Seismology and Geodynamics in Greece. *Geophys. Res. Abstr.* EGU Gen. Assem. 13, pp 2011-4840.

Hollenstein, C., Müller, M.D., Geiger, A., Kahle, H.G. (2008). Crustal motion and deformation in Greece from a decade of GPS measurements, 1993-2003. Tectonophysics 449, pp 17–40. doi:10.1016/j.tecto.2007.12.006

Hackl, M., Malservisi, R., Wdowinski, S. (2009). Strain rate patterns from dense GPS networks. Nat. Hazards Earth Syst. Sci. 9, pp 1177–1187.

Herring, TA., King, RW., &McClusky, SC. (2010). Documentation of the GAMIT GPS Analysis Software release 10.4. Dep Earth Planet Sci Massachusetts InstTechnol Cambridge, Massachusetts, pp 1-171.

Koukouvelas, I.K., and Aydin, A. (2002). Fault structure and related basins of the North Aegean Sea and its surroundings. Tectonics 21, pp 10-1-10–17. doi:10.1029/2001TC901037

Lazos, I., Kondopoulou, D., Chatzipetros, A., Pavlides, S., Bitharis, S., Pikridas, C. (2018a). Rotation rates of the South Aegean region, Greece, based on primary geodetic data - Comparison between geodetic and palaeomagnetic results. In: *Proc. Of 9th International INQUA Meeting on Paleoseismology, Active Tectonics and Archeoseismology (PATA)*. pp. 141–144.

Lazos, I., Stergiou, C.L., Chatzipetros, A., Pikridas, C., Bitharis, S., Melfos, V. (2018b). Active tectonics (extensional regime and rotations) and Tertiary mineralization occurrences within Central Macedonia, Greece. In: *Proc. Of 9th International INQUA Meeting on Paleoseismology, Active Tectonics and Archeoseismology (PATA)*. pp. 145–148.

Le Pichon, X., andAngelier, J. (1979). The hellenic arc and trench system: A key to the neotectonic evolution of the eastern mediterranean area. Tectonophysics 60, pp 1–42. doi:10.1016/0040-1951(79)90131-8

McClusky, S., Balassanian, S., Barka, A., Demir, C., Ergintav, S., Georgiev, I., Gurkan, O., Hamburger, M., Hurst, K., Kahle, H., Kastens, K., Kekelidze, G., King, R., Kotzev, V., Lenk, O., Mahmoud, S., Mishin, A., Nadariya, M., Ouzounis, A., Paradissis, D., Peter, Y., Prilepin, M., Reilinger, R., Sanli, I., Seeger, H., Tealeb, A., Toksöz, M.N., Veis, G. (2000). Global Positioning System constraints on plate kinematics and dynamics in the eastern Mediterranean and Caucasus. J. Geophys. Res. 105, pp 5695. doi:10.1029/1999JB900351

Mercier, J.-L., Carey-Gailhardis, E., Mouyaris, N., Simeakis, K., Roundoyannis, T., Anghelidhis, C. (1983). Structural analysis of recent and active faults and regional state of stress in the epicentral area of the 1978 Thessaloniki earthquakes (northern Greece). Tectonics 2, pp 577–600. doi:10.1029/TC002i006p00577

Mercier, J.L., Sorel, D., Vergely, P., Simeakis, K. (1989). Extensional tectonic regimes in the Aegean basins during the Cenozoic. Basin Res. 2, pp 49–71. doi:10.1111/j.1365-2117.1989.tb00026.x

Mountrakis, D., Tranos, M., Papazachos, C., Thomaidou, E., Karagianni, E., Vamvakaris, D. (2006). New neotectonic and seismological data about the main active faults and stress regime of Northern Greece. Geol. Soc. London, Spec. Publ. 260, pp 649–670.

Mountrakis, D. (2006). Tertiary and Quaternary tectonics of Greece, in: Special Paper 409: Postcollisional Tectonics and Magmatism in the Mediterranean Region and Asia. Geological Society of America, pp. 125–136. doi:10.1130/2006.2409(07)

Panagiotopoulos, D., Papadimitriou, E., Papaioannou, C., Scordilis, E., Papazachos, B. (1993). Source properties of the 21 Dec 1990 Goumenissa Earthquake in Northern Greece. In: *Proc. Of 2nd Congress Hellenic Geophysical Union.* pp. 286–296.

Pavlides, S.B., and Tranos, M.D. (1991). Structural characteristics of two strong earthquakes in the North Aegean: Ierissos (1932) and Agios Efstratios (1968). J. Struct. Geol. 13, pp 205–214. doi:10.1016/0191-8141(91)90067-S

Pavlides, S.B., Zouros, N.C., Chatzipetros, A.A., Kostopoulos, D.S., Mountrakis, D.M. (1995). The 13 May 1995 western Macedonia, Greece (KozaniGrevena) earthquake; preliminary results. Terra Nov. 7, pp 544–549. doi:10.1111/j.1365-3121.1995.tb00556.x

Pavlides, S., Caputo, R., Sboras, S., Chatzipetros, A., Papathanasiou, G. and Valkaniotis, S. (2010). The Greek Catalogue of Active Faults and Database of Seismogenic Sources. Bull. Geol. Soc. Greece, 43(1), pp 486-494.

Reilinger, R., McClusky, S., Vernant, P., Lawrence, S., Ergintav, S., Cakmak, R., Ozener, H., Kadirov, F., Guliev, I., Stepanyan, R., Nadariya, M., Hahubia, G., Mahmoud, S., Sakr, K., ArRajehi, A., Paradissis, D., Al-Aydrus, A., Prilepin, M., Guseva, T., Evren, E., Dmitrotsa, A., Filikov, S. V., Gomez, F., Al-Ghazzi, R., Karam, G. (2006). GPS constraints on continental deformation in the Africa-Arabia-Eurasia continental collision zone and implications for the dynamics of plate interactions. J. Geophys. Res. Solid Earth 111. doi:10.1029/2005JB004051

Robertson, A., and Dixon, J. (1984). Introduction: aspects of the geological evolution of the Eastern Mediterranean. Geol. Soc. London, Spec. Publ. 17, pp 1–74.

Sboras, S., Chatzipetros, A., Pavlides, S. (2017). North Aegean Active Fault Pattern and the 24 May 2014, Mw 6.9 Earthquake, in: Active Global Seismology: Neotectonics and Earthquake Potential of the Eastern Mediterranean Region. John Wiley & Sons, Inc., pp 239–272. doi:10.1002/9781118944998.ch9

Sboras, S., Chatzipetros, A., Pavlides, S., Karastathis, V., & Papadopoulos, G. (2016). EARTHQUAKE TRIGGERING EFFECT SCENARIOS DURING THE 2014 SEQUENCE IN CEPHALONIA AND 2015 EARTHQUAKE IN LEFKADA BROADER AREAS, IONIAN SEA, GREECE. Bulletin of the Geological Society of Greece, 50(1), pp 540-551. doi:http://dx.doi.org/10.12681/bgsg.11754

Sboras, S., 2012. The Greek Database of Seismogenic Sources: seismotectonic implications for North Greece, PhD Thesis, Università degli studi di Ferrara, Italy, pp 252.

http://www.unavco.org